Materials Science-Poland, 34(4), 2016, pp. 786-793
http://www.materialsscience.pwr.wroc.pl/
DOI: 10.1515/msp-2016-0122

DE GRUYTER OPEN

Structural, electrical and magnetic features of Kagomé $YBaCo_4O_7$ system

MASROOR AHMAD BHAT[1], R. A. ZARGAR[2,*], ANCHIT MODI[1], M. ARORA[3], N. K. GAUR[1]

[1]Department of Physics, Barkatullah University, Bhopal 462026, India
[2]Department of Physics, Jamia Millia Islamia, New Delhi 110025, India
[3]CSIR-National Physical Laboratory, Dr. K.S. Krishnan Marg, New Delhi 110012, India

Polycrystalline yttrium barium cobaltite ($YBaCo_4O_7$) powdered sample was prepared by conventional solid state reaction route using high purity yttrium oxide, barium carbonate and cobalt oxide. The as-prepared sample was characterized by XRD diffraction, SEM/EDAX, Raman analytical techniques, resistivity and magnetization measurements for structural, morphological, electrical and magnetic properties assessment. XRD pattern confirms the single phase formation of the sample without any impurity. SEM image shows the hexagonal growth of the crystal and EDAX spectrum reveals stoichiometric composition of as prepared sample. The variation in electrical resistivity from 90 K to 300 K follows the variable range hopping conductivity mechanism. The strong broad overlapped Raman peaks of Co–O and Y–O stretching and bending vibrations of tetrahedral CoO_4 with included components of YO_6 of octahedral symmetry are obtained at 542 cm^{-1}, 486 cm^{-1} and 636 cm^{-1}, 436 cm^{-1}, respectively. DC magnetic susceptibility exhibits very weak ferromagnetism below 80 K and does not obey Curie-Weiss law.

Keywords: *scanning electron microscopy (SEM); XRD analysis; DC magnetic susceptibility*

1. Introduction

The physical properties of mixed valence transition metal oxides can be tuned by interplay among charge, spin and orbital degrees of freedom interacting with crystal lattice [1, 2]. The geometrically frustrated hexagonal 114 phase in $YBaCo_4O_7$ compound contains CoO_4 tetrahedron present in alternating layers of Kagomé arranged in triangular arrays [3, 4]. Ba and O atoms form a close-packed structure with 4H (abac) stacking [3, 5]. Y and Co atoms occupy the octahedral and tetrahedral sites in the lattice, respectively. The CoO_4 tetrahedrons form a three-dimensional network by the corner sharing in a non-centrosymmetric $P6_3mc$ lattice. It has been reported on the basis of X-ray diffraction patterns of $ReBaCo_4O_7$ (Re = Lu, Yb, Tm) with a hexagonal $P6_3mc$ system [6]. On lowering temperature below 165 K, 180 K, and 230 K, these compounds exhibit structural phase transitions to orthorhombic system. The powder X-ray diffraction patterns of low-temperature phases are indexed under orthorhombic system with $Cmc2_1$ symmetry, a subgroup of $P6_3mc$ space group. Such systems are also reported in oxygen deficient phase in $Ba_2Er_2Zn_8O_{13}$ [7]. Recent studies of oxygen stoichiometry in 114 phase have revealed the existence of a large oxygen non-stoichiometry going from O_7 to $O_{8.5}$ [8, 9], i.e. the cobalt oxidation state (v_{Co}) varies from 2.25 to 3. In contrast, $LnBaCo_4O_7$ (Ln = Lu, Yb, Tm), the O_7 phases are characterized by structural transitions (space group $P6_3mc$ to $Cmc2$) with characteristic temperature (T_S) increasing from T_S = 165 K (Ln = Lu) to T_S = 230 K (Ln = Tm) as the Ln^{3+} ionic radius decreases [6]. The origin of this behavior is still not clear and therefore is a topic of intense investigation. It was discussed in [10] that this transition was caused by the tendency to optimize the Ba^{2+} bonding, especially at the high temperature phase. Another reason for this transition is the partial charge ordering of Co^{2+} and Co^{3+} at the Kagomé (Co^{2+}) and triangular (Co^{3+}) sites [6].

*E-mail: rayeesphy12@gmail.com

Magnetic structure of $YBaCo_4O_7$ has been studied recently by neutron diffraction technique [11, 12]. In the literature [12], it was shown that this system undergoes the structural transition at 313 K. On the other hand, $YbBaCo_4O_7$ undergoes a structural transition from trigonal (P31c) to orthorhombic (Pbn21) below 175 K [13].

Even though the basic crystal structure of the oxygen-deficient form of $YBaCo_4O_{7+\delta}$ ($\delta = 0$) was determined already in 2002 [3], much less is known about the crystal structure(s) of the oxygenated phase(s). The parent $YBaCo_4O_7$ structure is of hexagonal symmetry (space group $P6_3mc$ [3] or P31c [13]) and consists of two kinds of corner-sharing CoO_4 tetrahedrons (with a ratio of 1:3) located in separate, alternately stacked layers of triangular and Kagomé types. Recently Chmaissem et al. [14] described in a satisfactory manner the crystal structure of their $YBaCo_4O_{8.1}$ sample in the orthorhombic space group $Pbc2_1$ on the basis of high-resolution neutron and synchrotron X-ray powder diffraction data. In their structure model, Co atoms occupy both corner-sharing tetrahedral and edge-sharing octahedral sites.

Recently, Co-based compounds have intensively been investigated due to the existence of intriguing magnetic properties [15]. The most representative member of such cobalt oxide systems is the spinel Co_3O_4 which features antiferromagnetic ordering [16]. Apart from this, Co-rich quaternary systems like Ln_2BaCoO_5 (Ln = Y, Sm, Er) have also gained enormous interest because of their similarity to the cuprate Y_2BaCuO_5 discovered in the high temperature superconductor $YBa_2Cu_3O_{7-\delta}$ [17, 18]. In addition, it was also established that Co-rich compounds, such as $(Sr,Ca,Ln)_3Co_2O_{6+\delta}$ (Ln = Sm–Ho and Y) exhibit long range antiferromagnetism or spin-glass properties [19]. These double perovskite compounds LnBa and Co_2O_5 proved to be antiferromagnetic [20]. On the other hand, the new type of magnetic compound $YBaCo_4O_{7+\delta}$, denoted 114, was reported to exhibit an unusual magnetic behavior, which resembled that of spin-glass [21].

The semiconducting character of the 114-phase (from low to high temperatures) has been clearly established from various reports but the electronic transport process has not been systemically analyzed so far. Several models have been proposed to study the temperature dependence of electrical resistivity of these compounds. Therefore, motivated by these facts, we thought it is pertinent to study in this paper the physical properties of these compounds. Moreover, there is a global need to know about the structural electronic and magnetic properties of these compounds in order to explore their usage in various device applications.

2. Experimental

The polycrystalline samples of $YBaCo_4O_7$ were prepared by the conventional solid state reaction method. The high purity chemicals Y_2O_3 (99.9 %), $BaCO_3$ (99.999 %) and Co_4O_7 (99.99 %) were taken for synthesis purpose. These starting compounds were grinded for 2 hours before heating in air in a muffle furnace at 950 °C for 12 hours to complete decarbonisation reaction, i.e. decomposition of barium carbonate to barium oxide in the ground mixture of three precursors. The calcined powders were thoroughly ground and pressed into cubical pellets of dimension (2 mm × 2 mm × 10 mm). The pellets were further heated to 1130 °C at a rate of 100 °C/h. and then heated at this temperature for 24 hours. Then, these samples were cooled to ambient temperature during 12 hours. This process completed solid state reaction with desired homogenous single phase stoichiometry without any impurities or unreacted precursor phase. X-ray powder diffraction patterns were recorded using CuKα radiation (X-ray wavelength: 1.54056 Å) in the 2θ range of 20° to 100° using Bruker Advanced-D8 powder X-ray diffractometer. The scanning speed and steps were 2°/minute and 0.02° of 2θ, respectively. The rotating anode X-ray generator was operated at 46 kV and 200 mA. A graphite (0 0 2) monochromator was used and the widths of the divergent slit, scatter slit and the receiving slit were 0.50, 0.50, 0.15 mm, respectively. Rietveld refinement was carried out using the FullProof package. The refined parameters included 2θ-zero, spectrum background fitted by 6-polynomial function, lattice

parameters, atomic coordinates and thermal parameters. The pseudo-Voigt profile shape parameters were used. The JEOL JSM-6700 working at room temperature and operating at 20 kV was used to record the microstructural image of the compound. Perkin Elmer FT-Raman spectrophotometer (Model: GX 2000) was used for recording Raman spectra in 1600 cm^{-1} to 100 cm^{-1} region at the ambient temperature at 4 cm^{-1} instrumental resolution. The zero and high magnetic field electrical resistances were measured by using standard four probe method in the temperature range of $5\ K \leqslant T \leqslant 300\ K$, using liquid He coolant cryostat and superconducting magnet. The magnetization measurements were carried out in Zero Field Cooled (ZFC), Field Cooled Warming (FCW) and Field Cooled (FC) as a function of temperature (T) at magnetic field of 1 T using a Quantum Design SQUID magnetometer. The magnetic hysteresis loops were recorded at 3 K, 50 K and 300 K from 0 T to 8 T, respectively.

3. Results and discussion

3.1. XRD study

XRD pattern of the $YBaCo_4O_7$ sample recorded at ambient temperature shown in Fig. 1 was refined with the Rietveld refinement method using the fullproof program [22]. The refinement confirmed the single phase hexagonal structure with $P6_3mc$ space group and no evidence for impurities was found within the detection limit of the X-ray diffractometer. The unit cell parameters a and c of prepared $YBaCo_4O_7$ are 6.2873 Å and 10.2533 Å respectively, that is very close to the reported values [23] which together with the other parameters calculated from this pattern are summarised in Table 1.

3.2. SEM/EDAX analysis

Scanning electron microscopy with EDAX accessory has been used to examine the microstructure and composition of the pellet at the centre which provides a better insight and accuracy of the grain development than at the top and bottom surfaces. The grain morphology is depicted in Fig. 2a.

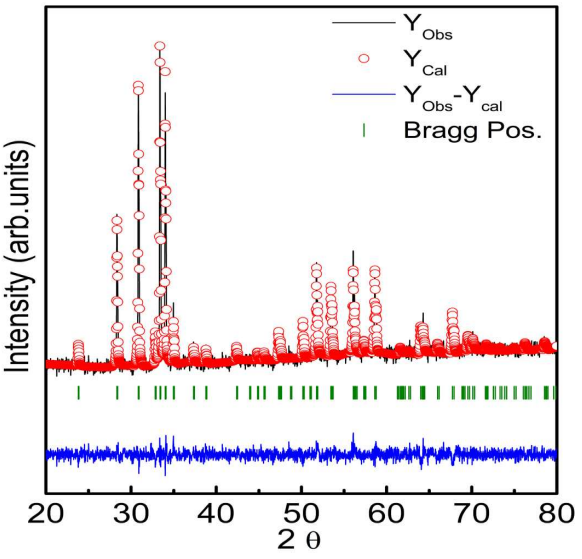

Fig. 1. XRD pattern of $YBaCo_4O_7$ with Reitveld refinement.

From the image it is clear that the hexagonal grains having the sizes of the order of 5 μm are well defined and distributed homogeneously across the structure. The fine network distribution among the grains is due to smooth mixing of different constituents in a fine network aggregate form and is a feature responsible for electronic and magnetic properties.

The compositional analysis confirmed by EDAX, displayed in Fig. 2b, shows the elemental composition for Y, Ba, and Co close to the stoichiometric value as shown in Table 2. The EDX patterns clearly give an indication of the structural phase purity in the prepared high quality sample that supports the XRD result also.

3.3. Raman spectra

Fig. 3 shows the Raman spectra of $YBaCo_4O_7$ (hexagonal space group P63mc) recorded at room temperature in the 1600 cm^{-1} to 100 cm^{-1} region. The group theory predicts the following irreducible representation as [24]:

$$\Gamma_{\text{optical}} = 4A_1 + A_2 + 4B_1 + 1B_2 + 5E_1 + 5E_2 \quad (1)$$

where A_1, E_1 and E_2 are Raman active (14 modes) and A_1 and E_1 are infrared-active (9 modes), while A_2, B_1 and B_2 are optically inactive.

Table 1. $YBaCo_4O_7$ different XRD parameters; space group - $P6_3mc$, a = 6.2874 Å, c = 10.2533 Å, volume = 660.9953 $Å^3$, $\chi^2 = 1.351$, $R_{wp} = 19.5$, $R_{exp} = 16.7$.

Atom	Atom site multiplicity	X	Y	Z	Occupancy
Y	2b	0.66667	0.33334	0.87855	0.16667
Ba	2b	0.66667	0.33334	0.50000	0.16667
Co_1	2a	0.00000	0.00000	0.44028	0.16667
Co_2	6c	0.18987	0.85218	0.67724	0.50000
O_1	6c	0.38893	0.47100	0.71181	0.50000
O_2	2a	0.00000	0.00000	0.22156	0.16667
O_3	6c	0.12436	0.80951	0.54566	0.50000

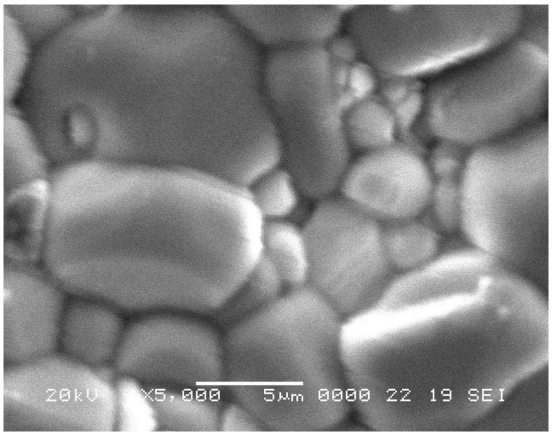

(a)

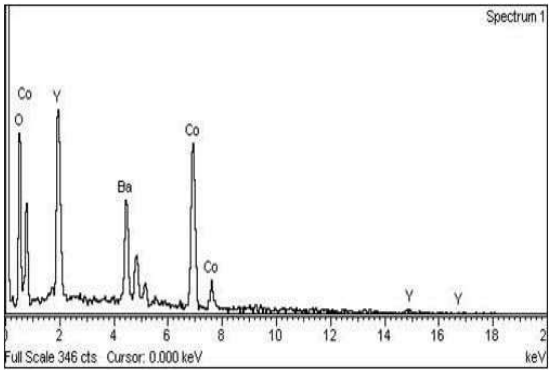

(b)

Fig. 2. (a) SEM image and (b) EDX pattern of $YBaCo_4O_7$.

Table 2. Elemental composition details in wt.% and at.% of $YBaCo_4O_7$ obtained from EDX pattern.

Element	wt.%	at.%
O K	30.42	68.66
Co K	29.01	17.77
Y L	20.27	8.23
Ba L	20.30	5.34
Total	100.00	100.00

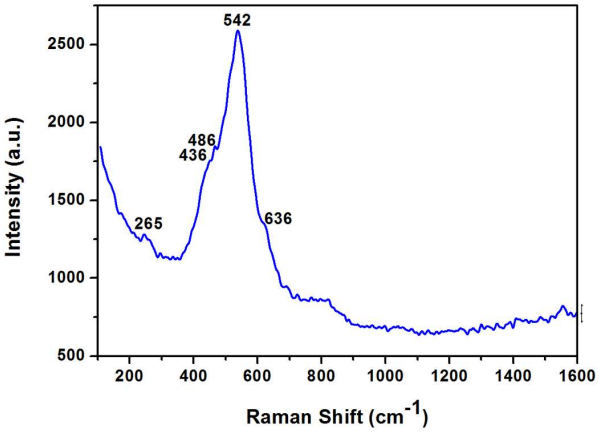

Fig. 3. Raman spectrum of $YBaCo_4O_7$ in the 100 cm^{-1} to 1600 cm^{-1} region.

The most intense mode at 542 cm^{-1} could be the symmetric stretching mode of the CoO_4 tetrahedron and the lowest frequency mode at 255 cm^{-1} arises from its bending vibrations. The strong broad overlapped Raman peak of O–Y–O stretching and bending vibrations of YO_6 of octahedral symmetry are obtained as included components at 636, cm^{-1} 436 cm^{-1}, respectively. The only report available on Raman spectra of the bulk $YBCo_4O_7$ by Izquierdo et al. [25] and our Raman spectra are in good agreement with the broad band centred at 542 cm^{-1} [26].

3.4. Resistivity measurement

The electrical response is depicted in Fig. 4 where we have shown the resistivity of $YBaCo_4O_7$ compound measured at magnetic fields of 0 and 8 Tesla (T). We have measured the temperature dependence of the resistance of $YBaCo_4O_7$ pellets upon cooling and warming cycles. There is no change observed between these two processes. The semiconducting behavior of these compounds, which is not affected by 8 T field, is clearly seen in the measured temperature range [27].

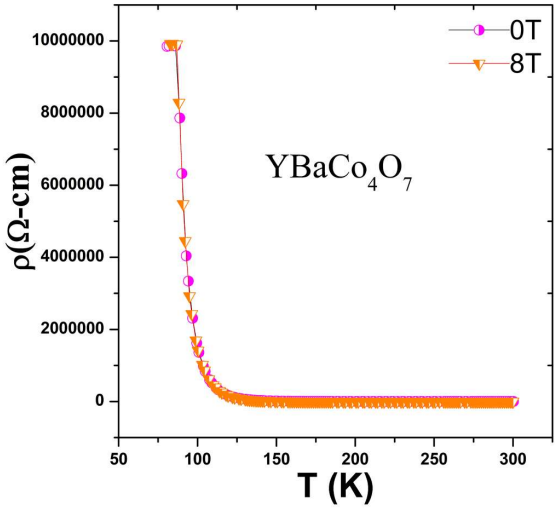

Fig. 4. Resistance vs. temperature at 0 T and 8 T magnetic field.

The suppression of any kind of transition is probably due to the presence of extra oxygen in the structure which tends to increase locally the coordination of the cobalt cations with formal oxidation state $Co^{2.25+}$ ($\delta = 0$). This, in turn, creates locally a more disordered crystallographic structure for 114 compounds $YBaCo_4O_7$ which seems not to be compatible with the cobalt magnetic ordering [28]. Indeed, by increasing the hole concentration in the $O_{7+\delta}$ phase, the extra oxygen atoms would hinder the triangular arrangement for the magnetic moments of the tetrahedrally coordinated CoO_4 since new polyhedra are created. This suppresses the transition. On the other hand, it is probable that a structural transition takes place at a local scale. However, if a structural transition had happened at a local scale, it would have been very difficult to detect by normal XRD or transport measurements.

The electrical transport mechanism was tested using different models which depict the temperature dependence of the electrical resistivity. The conventional Arrehenius plots:

$$\rho(T) = Ce^{(E/k_BT)} \tag{2}$$

suggests simple thermal activation transport [29]. While considering the small polaron hopping conduction mechanism, the behavior of electrical resistivity versus temperature should be expressed as $\rho(T) = CTe^{(E/k_BT)}$) [28]. Another approach is the Mott's VRH model in which the dependence of resistivity on the temperature is given by [30]:

$$\rho(T) = \rho_0 \exp(T^0/T)^{1/4} \tag{3}$$

Here, ρ_0, T^0 and n are constants. The quantity 1/4, depends on the dimensionality D and, in some compounds, on the temperature range. In the study of our sample, the resistivity data measured on the $YBaCo_4O_7$ pellets seemed to obey the VRH model. In Fig. 5 the fitting is shown for variable range hopping (VRH) model under 0 T and 8 T field. By plotting the experimental data $\rho(T)$ as $\rho(T) = C(T)\exp(E/k_BT)$ in the temperature range of 300 K to 20 K, it is readily recognized that neither simple thermal activation nor small polaron hopping conduction describe well the electronic transport in the reported pellets. In the present study of $YBaCo_4O_7$ compound, only the VRH model is well fitted in the whole measured temperature range 300 K to 20 K, therefore we have shown only the fitting data for VRH model. The VRH model is promptly verified. From Fig. 5 it can be observed that a linear fit is obtained in all the compounds of this series, indicating that the Mott's 3D-VRH mechanism is the most prevalent conduction mechanism in these compounds for this temperature range. The Mott's parameter (T^0) and the density of states ($N(E_F)$) were calculated for the samples studied in about 0 T and 8 T fields. The characteristic temperature T^0 is related to the parameter ξ through the expression:

$$k_BT^0 = 24/\pi N(E_F)\xi^3 \tag{4}$$

where $N(E_F)$ is the density of states at the Fermi level [31]. By taking $\xi \approx c = 10.254$ Å, $N(E_F)$ was estimated for these polycrystalline samples. The fact that the electrical resistivity may be described by VRH model, points out to the presence of disorder induced localization of charge carriers in the samples. VRH mechanism normally occurs only in the low-temperature region (below room temperature), wherein the energy is insufficient to excite the charge carriers across the Coulomb gap. Hence, conduction is accomplished by hopping within a small region ($\sim k_B T$) in the vicinity of E_F. In this region, the density of states remains almost constant [13]. The values are closer to the expected values for transition metal compounds.

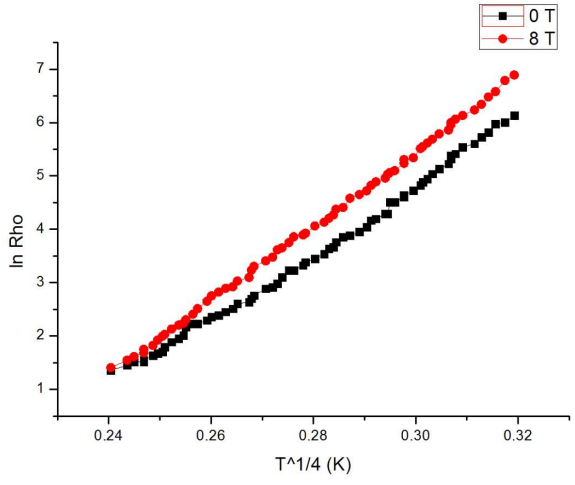

Fig. 5. lnρ vs. $T^{-1/4}$ ($K^{-1/4}$) at 0 T and 8 T with linear fit.

The Mott's parameter (T^0) and the density of states $N(E_F)$ were calculated for the sample studied in about 0 T and 8 T fields. In Table 1 the calculated values for T^0 and $N(E_F)$ are also reported. The typical value of T^0 and $N(E_F)$ are about 3.4×10^8 K and 2.4×10^{17} eV^{-1} cm^{-3}, respectively.

3.5. Magnetization

The DC magnetic susceptibility (M/H) measurements for $YBaCo_4O_7$ were carried out by using SQUID magnetometer as shown in Fig. 6. In this paper, we have shown the magnetization of $YBaCo_4O_7$ compound measured at 1 Tesla (T) magnetic field. From 80 K to 300 K, the data do not obey a Curie-Weiss relationship. We have collected our data for zero field cooled (ZFC), field cooled (FC) and for field cooled warming (FCW), however during the analysis of the results we have not found any difference between FCW and FC data, as shown in the Fig. 6. Enlargement of ZFC, FC and FCW shown in the inset of Fig. 6, shows clear lack of hysteresis at T_C here. The FC curve is noticeably different than the ZFC data. The compound $YBaCo_4O_7$ shows ferromagnetic-like transition that appears at about 91 K with large irreversibility between ZFC and FC curves as shown in Fig. 6. This type of behavior has also been reported in Huq et al., [13]. The ZFC curve also shows another magnetic transition at $T_C = 40$ K for this pure sample.

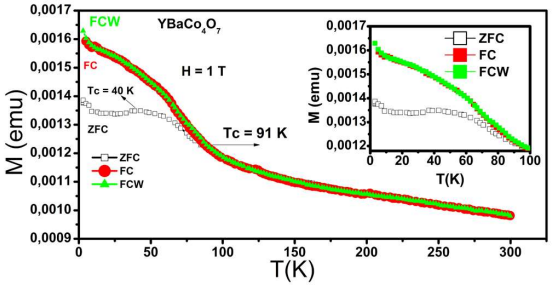

Fig. 6. M (emu) vs. T (K) for ZFC, FC and FCW for $YBaCo_4O_7$ under 1 T magnetic field.

In the present literature the magnetization data has been reported but still it is not clear. It is obvious that the sample $YBaCo_4O_7$ exhibits a complicated inhomogeneous magnetic phase. Interestingly, we have also found ferromagnetic transition at $T_c = 80$ K. Super-exchange couplings build up a geometrically frustrated substructure in the planes of Co_2 and as the temperature is lowered, the combination between super-exchange and double-exchange causes the magnetic system to degenerate. Further, on cooling, the strength of the double-exchange diminishes, since the electrons do not have enough energy (heat) to hop between the Co atoms. At the same time, the super-exchange starts to couple in more directions and dominates at lower temperature. On the basis of above discussion it is established that the overall magnetic interactions can be described as those of a glassy

disordered antiferromagnetic, where double-exchange phenomenon dominates at higher temperatures and super-exchange at the lower ones and they compete through the whole measured temperature range on the frustrated lattice. It has also been exhibited for other systems, but the magnetic order in those cases was confined within the planes, prohibiting long-range order to occur. To get additional insight into this high state field we have carried out isothermal magnetization at three different temperatures for all the samples at 3 K, 50 K and 300 K and the results are shown in Fig. 7. The M(H) curve measured for all the three assumed temperatures is linear, and an irreversible characteristics have been found at all magnetic fields measured at about 0 T and 8 T. The M (H) measured data confirms that no hysteresis of magnetization has been found in these compounds. The magnetization value at these three different temperatures is small and does not change for the wide range of temperatures.

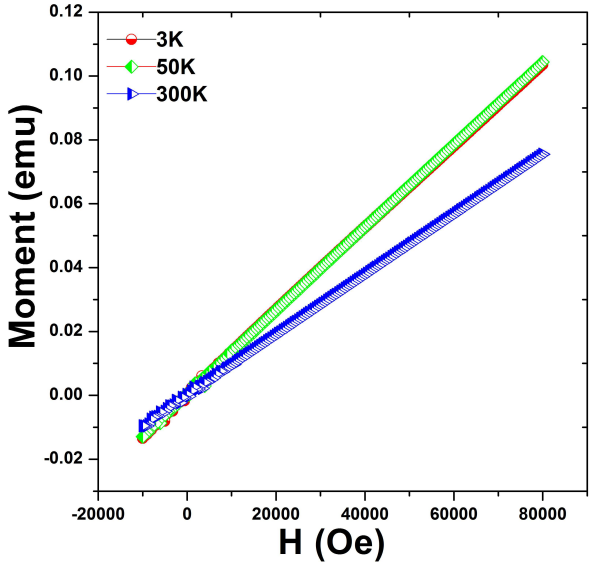

Fig. 7. Isothermal magnetization moment (emu) vs. magnetic field H (Oe).

The effective moment value calculated from the fitting procedure for pure $YBaCo_4O_7$ sample is 11.68 μ_{eff} (not shown here), which is larger than the value given by Lu et al. [33], i.e. 9.8 μ_{eff}. This variation is due to the difference in measured temperature range. In the present work we have performed the measurements below 300 K and in [33] in the range of 300 to 400 K. Such large μ_{eff} value indicates that there exist some short range magnetic interaction in the high temperature in our measured paramagnetic (PM) range.

4. Conclusions

We have prepared and carried out successfully the investigation of physical properties of frustrated $YBaCo_4O_7$ system by using solid state reaction method. Rietveld analysis has shown the existence of a single phase without any secondary impurity which indicates the high level crystal formation of $YBaCo_4O_7$ compound. The grains are distributed homogeneously in their hexagonal form and the composition is uniform throughout the measurement range. The Raman bands have been assigned to Y–O and Co–O bonds in tetrahedral and octahedral coordination, respectively. The sample shows semiconducting nature in the whole studied temperature range and obeys Mott's VRH model fit in both fields of 0 T and 8 T. The ferromagnetic like behavior is evident at the expense of antiferromagnetism due to the dominance of intrinsic double exchange mechanism.

Acknowledgements

Masroor Ahmad Bhat is thankful to the University Grants Commission (UGC), New Delhi for providing the financial support under the Project No. F.7-19/2007 (BSR). We express our sincere thanks to Dr. Mukul Gupta, Dr. Rajeev Rawat, Dr. D. M. Phase and Dr. Alok Banerjee IUC- DAE Indore for helping us to carry out the characterizations and fruitful discussions. R.A. Zargar is also thankful to Prof. Saeeduddin Head of Department of Physics JMI, for his continuous cooperation and encouragement.

References

[1] TERASAKI I., SASAGO Y., UCHINOKURA K., *Phys. Rev. B*, 36 (1997), R12685.
[2] MASSET A.C., MICHEL C., MAIGNAN A., HERVIEU M., TOULEMONDE O., STUDER F., RAVEAU B., *Phys. Rev. B*, 62 (2000), 166.
[3] VALLDOR M., ANDERSON M., *Solid State Sci.*, 4 (2002), 923.
[4] SODA M., YASUI Y., MOYOSHI T., SATO M., IGAWA N., KAKURAI K., *J. Phys. Soc. Jpn.*, 75 (2006), 054707.
[5] VALLDOR M., *Solid State Sci.*, 6 (2004), 251.
[6] NAKAYAMA N., *J. Magn. Magn. Mater.*, 300 (2006), 98.

[7] RABBOW C.H., MULLER-BUSCHBAUM H.K., *Z. Anorg. Allg. Chem.*, 620 (1994), 527.
[8] TSIPIS E.V., KHARTON V.V., FRADE J.R., NUNEZ P., *J. Solid State Electr.*, 9 (2005), 547.
[9] KARPPINEN M., YAMAUCHI H., OTAMI S., FUJITA T., MOTOHASHI T., HUANG Y.H., VALKEAPÄÄ M., FJELLAG H., *Chem. Mater.*, 18 (2006), 490.
[10] HUQ A., MITCHELL J.F., ZHENG H., CHAPON L.C., RADAELLI P.G., KNIGHT K.S., STEPHENS P.W., *J. Solid State Chem.*, 179 (2006), 1136.
[11] SODA M., YASUI Y., MOYOSHI T., SATO M., IGAWA N., KAKURAI K., *J. Phys. Soc. Jpn.*, 75 (2006), 054707.
[12] CHAPON L.C., RADAELLI P.G., ZHENG H., MITCHELL J.F., *Cond.-Mat. Mtrl.-Sci.*, 5 (2006), 307.
[13] HUQ A., MITCHELL J. F., ZHENG H., CHAPON L.C., RADAELLI P.G., KNIGHT K.S., STEPHENS P.W., *J. Solid State Chem.*, 179 (2006), 1136.
[14] CHMAISSEM O., ZHENG H., HUQ A., STEPHENS P.W., MITCHELL J.F., *J. Solid State Chem.*, 181 (2008), 664.
[15] PEKALA M., MUCHAB J., BARANC M., TROYANCHUKD I., KRZYMANSKA B., SZYMCZAK H., *J. Magn. Magn. Mater.*, 292 (2005), 385.
[16] ROTH W.L., *J. Phys. Chem. Solids*, 1 (1964), 25.
[17] MEVS H., MÜLLER-BUSCHBAUM H., *Z. Anorg. Allg. Chem.*, 172 (1989), 574.
[18] MEVS H., MÜLLER-BUSCHBAUM H., *Z. Anorg. Allg. Chem.*, 128 (1989), 573.
[19] YAMAURA K., HUANG Q., CAVA R.J., *J. Solid State Chem.*, 146 (1999), 277.
[20] VOGT T., WOODWARD P.M., KAREN P., HUNTER B.A., HENNING P., MOODENBAUGH A.R., *Phys. Rev. Lett.*, 84 (2000), 13.
[21] TSIPIS E.V., KHALYAVIN D.D., SHIRYAEV S.V., REDKINA K.S., NUŃEZ P., *Mater. Chem. Phys.*, 33 (2005), 92.
[22] WILES D.B., YOUNG A., *J. Appl. Crystallogr.*, 14 (1981), 149.
[23] VALLDOR M., ANDERSON M., *Solid State Sci.*, 4 (2002), 923.
[24] NITHYA R., KUMARY T.G., RAVINDRAN T.R., *AIP Adv.*, 3 (2013), 022115.
[25] IZQUIERDO J.L., MONTOYA J.F., GOMEZ A., PAUCAR C., MORAN O., *Solid State Sci*, 12 (2010), 2073.
[26] CHAPON L.C., RADAELLI P.G., ZHENG H., MITCHELL J.F., *Phys. Rev. B*, 74 (2006), 172401.
[27] MAIGNAN A., CAIGNAERT V., PELLOQUIN D., HÉBERT S., PRALONG V., HEJTMANEK J., KHOMSKII D., *Phys. Rev. B*, 74 (2006), 165110.
[28] WILSON M.L., BYERS J.M., DORSEY P.C., HORWITZ J.S., CHRISEY D.B., OSOFSKY M.S., *J. Appl. Phys.*, 81 (1997), 4971.
[29] TERESA J.M. DE, DÖRR K., MÜLLER K.H., SCHULTZ L., CHAKALOVA R.I., *Phys. Rev. B*, 58 (1998), R5928.
[30] MOTT N.F., *Conduction in Non-Crystalline Materials*, Clarendon Press, New York, 1993.
[31] JANA D., FORT J., *Physica B*, 344 (2004), 62.
[32] GROHOL D., MATAN K., CHAO J.H., LEE S.H., LYNN J.W., NOCERA D.G., LEE Y.S., *Nat. Mater.*, 4 (2005), 323.
[33] LU W. J., SUN Y.P., ANG R., ZHU X.B., SONG W.H., *Phys. Rev. B.*, 75 (2007), 014414.

Received 2016-02-13
Accepted 2016-10-25